Event-Triggered Filter Design Based on Average Measurement Output for Networked Unmanned Surface Vehicles

Zhou Gu, *Member, IEEE*, Choon Ki Ahn, *Senior Member, IEEE*, Shen Yan, Xiangpeng Xie, *Member, IEEE*, and Dong Yue, *Fellow, IEEE*

***Abstract*—This brief addresses the event-triggered H_∞ filtering problem for networked unmanned surface vehicles (USVs) subject to transmission delays. First, a novel event-triggered scheme based on the average measurement output (AMO) is proposed for scheduling the network transmissions of sensor measurements from a USV. Unlike traditional event-triggering conditions that adopt only the current measurement information, an average of consecutive sensor measurements over given time period T is used to verify the triggering condition. This allows the triggering scheme to employ historical measurements and make more reasonable decisions regarding network transmissions. As a consequence, the proposed triggering scheme has the potential to avoid unexpected events arising from stochastic disturbance and noise or malicious attacks. To solve the filtering problem, AMO-based event-triggered H_∞ filtering is then developed. Sufficient design criteria are also derived, from which the filter gain parameters can be readily determined. The efficacy of the proposed filter design method is illustrated via simulations using practical USV parameters.**

***Index Terms*—Event-triggered scheme, filter design, average measurement, unmanned surface vehicles.**

I. INTRODUCTION

UNMANNED surface vehicles (USVs) have been widely employed for commercial enterprises, scientific research, civil applications, and military use due to their low cost, high autonomy, and general usefulness for a wide range of activities [1]. Over the past few decades, in order to produce more intelligent USV frameworks that require less human control while offering higher reliability and accuracy, there has been significant research on improving their dynamic behavior and the accuracy of measurements and signal estimation [2], [3]. This has led to a significant volume of interesting results being reported for USVs. For example, the authors in [4] developed a reconfigurable disturbance compensation mechanism for USVs to extend their mission duration and enhance their accommodative capabilities. In [5], trajectory tracking of a USV in the presence of uncertainty and disturbance using single-hidden-layer feed forward network technology was investigated. However, many of these results have depended heavily on the reliability of the signals obtained from individual USVs. Therefore, the observation, filtering, and estimation of these signals have gained considerable research attention. For example, the authors in [6] developed an integral sliding mode control strategy for a USV by estimating the unmeasured velocity and unknown disturbances. In [7], a second-order nonlinear filter was designed to compensate for the magnitude and rate saturation of the rudder. A lateral dynamics-based fuzzy observer has also been established to simultaneously estimate the vehicle steering and side slip angles of a USV [8].

Generally, a wireless network is required for the exchange of information among USVs distributed over a wide area. As such, challenging issues such as optimizing the network bandwidth, reducing network-induced delays, and extending the battery life need to be addressed when USVs employ wireless network communication. Time-triggered schemes (TTSs) have been widely employed in traditional communication approaches. However, under a TTS, the transmission data includes a significant volume of redundant data, which may waste the limited network bandwidth and computational resources and reduce the battery life. Therefore, event-triggered scheme (ETSs) have attracted significant recent attention [9], [10], [11], [12]. Under an ETS, tasks can be executed under less control updating, solving the problem of redundant transmissions. For example, in [13], an ETS was developed for distributed networked control systems subject to packet losses and transmission delays and greatly reduced the volume of transmitted data. An integral-based ETS was presented in [14] for a system with observer-based output feedback. However, Zeno behavior is difficult to avoid under these schemes. A continuous memory-based ETS was investigated by introducing a constant scalar for the H_∞ filtering of USVs in [15]. Using this scheme, uniformly ultimately

Manuscript received 1 February 2022; revised 13 April 2022; accepted 11 May 2022. Date of publication 16 May 2022; date of current version 30 August 2022. This work was supported in part by the National Natural Science Foundation of China under Grant 62022044 and Grant 62103193; in part by the Jiangsu Natural Science Foundation for Distinguished Young Scholars under Grant BK20190039; and in part by the National Research Foundation of Korea (NRF) Grant funded by the Korea Government (Ministry of Science and ICT) under Grant NRF-2020R1A2C1005449. This brief was recommended by Associate Editor H. Dong. *(Corresponding authors: Choon Ki Ahn; Xiangpeng Xie.)*

Zhou Gu and Shen Yan are with the College of Mechanical and Electronic Engineering, Nanjing Forestry University, Nanjing 210037, China (e-mail: gzh1808@163.com; yanshenzdh@gmail.com).

Choon Ki Ahn is with the School of Electrical Engineering, Korea University, Seoul 136-701, Republic of Korea (e-mail: hironaka@korea.ac.kr).

Xiangpeng Xie and Dong Yue are with the Institute of Advanced Technology, Nanjing University of Posts and Telecommunications, Nanjing 210023, China (e-mail: xiexiangpeng1953@163.com; medongy@vip.163.com).

Color versions of one or more figures in this article are available at https://doi.org/10.1109/TCSII.2022.3175221.

Digital Object Identifier 10.1109/TCSII.2022.3175221

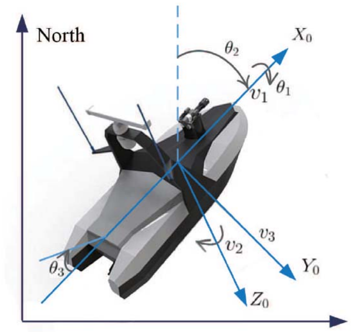

Fig. 1. Coordinate system for a USV on the planar plane.

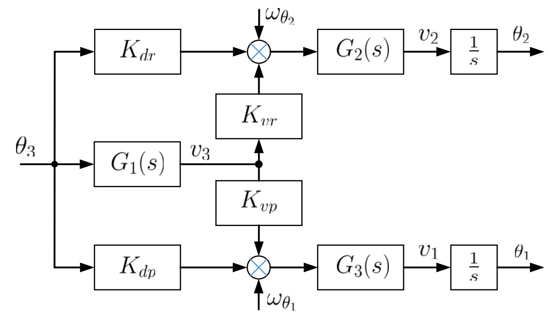

Fig. 2. Block diagram for a USV.

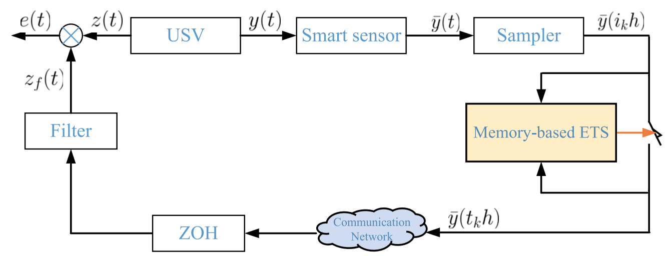

Fig. 3. AMO-based event-triggered filtering for a USV.

bounded filter design conditions were obtained instead of asymptotically stable conditions. Sampling-based ETSs are an effective and simple approach to avoid Zeno behavior. However, the information between the continuous sampling instants is inevitably lost. Therefore, determining how to use the information lost using this sampling approach while avoiding Zeno behavior is the main motivation of this brief.

Inspired by the observations above, this brief investigates an average measurement output (AMO)-based ETS for USVs within a wireless communication network to reduce the volume of transmitted data and to increase the battery life. The main contributions of this brief can be summarized as follows.

(1) The AMO of a USV over a given period is used as an element in the proposed ETS. This means errors associated with the triggering conditions are incorporated into the AMO rather than the output at the sampling instant. As a result, unexpected transmissions caused by disturbance and noise can be reduced.

(2) Periodical sampling for the AMO and an ETS for AMO transmission are adopted. Information loss can be reduced because the transmission signal includes historical information, thus improving the filtering performance of the USV. In addition, Zeno behavior can be avoided.

Notations: $\mathbf{He}\{X\}$ denotes $X + X^T$.

II. Problem Statement

In this brief, AMO-based filtering for USVs is investigated. We first introduce a motion model for a USV, the AMO-based ETS, and the filter modeling, then we present the filter design for the USV.

The earth- and body-fixed coordinates of the USV are presented in Fig. 1, where θ_1, θ_2 and θ_3 are the roll, heading and rudder angle, respectively, v_1, v_2 and v_3 are the roll, yaw and sway velocity, respectively. Fig. 2 displays a block diagram of the USV, where ω_{θ_1} and ω_{θ_2} represent the disturbance induced by θ_1 and θ_2, respectively. In Fig. 2, $G_1(s) = \frac{K_{dv}}{T_v s+1}$, $G_2(s) = \frac{1}{T_r s+1}$, and $G_3(s) = \frac{s\omega_n^2}{s^2+2\zeta\omega_n s+\omega_n^2}$. $K_{dv}, K_{dr}, K_{dp}, K_{vr}$ and K_{vp} are the respective gains, T_r, and T_v are time constants, and ζ and ω_n are the damping ratio and the undamped natural frequency, respectively.

Given $x(t) = [\theta_1\ \theta_2\ v_1\ v_2\ v_3]^T$ and $\omega(t) = [\omega_{\theta_1}\ \omega_{\theta_2}]$, we can obtain the planar dynamic model for the USV as follows:

$$\dot{x}(t) = Ax(t) + Bu(t) + \mathcal{B}\omega(t), \tag{1}$$

where

$$A = \begin{bmatrix} 0 & 0 & 1 & 0 & 0 \\ 0 & 0 & 0 & 1 & 0 \\ -\omega_n^2 & 0 & -2\zeta\omega_n & 0 & \omega_n^2 K_{vp} \\ 0 & 0 & 0 & -\frac{1}{T_r} & \frac{K_{vr}}{T_r} \\ 0 & 0 & 0 & 0 & -\frac{1}{T_v} \end{bmatrix}, B = \begin{bmatrix} 0 \\ 0 \\ \omega_n^2 K_{dp} \\ \frac{K_{dr}}{T_r} \\ \frac{K_{dv}}{T_v} \end{bmatrix},$$

$$\mathcal{B} = \begin{bmatrix} 0 & 0 & \omega_n^2 & 0 & 0 \\ 0 & 0 & 0 & 0 & \frac{1}{T_r} \end{bmatrix}^T.$$

The USV system in (1) is stabilized by a local feedback controller $u(t) = \theta_3(t) = Kx(t)$; that is $A+BK \triangleq \mathcal{A}$ is Hurwitz stable. The closed-loop USV system is then given by

$$\begin{cases} \dot{x}(t) = \mathcal{A}x(t) + \mathcal{B}\omega(t) \\ y(t) = \mathcal{C}x(t) \\ z(t) = \mathcal{E}x(t) \end{cases} \tag{2}$$

To produce a better filtering performance for the networked USVs, we develop a filter with the structure shown in Fig. 3, where ZOH is a zero-order hold, and the smart sensor is responsible for calculating the AMO given in (3).

Applying the Simpson's rule [16], the AMO of the USV is approximately

$$\begin{aligned} \bar{y}(t) &= \frac{1}{T}\int_{t-T}^{t} y(s)ds \\ &\approx \frac{1}{6}\big[y(t) + 4y(t-T/2) + y(t-T)\big]. \end{aligned} \tag{3}$$

Remark 1: In (3), T is the time scale of the sliding window used to calculate the AMO of the USV from the current time t to $t-T$. To ensure the filter input with less information loss, smart sensor is introduced before the sampler, which is different from the method in [11]. T satisfies $T > h$, where h is the sampling period. However if T is too large, the sensitivity of the filtering system to the transient USV output will be low.

The following novel AMO-based ETS is designed to determine the sampling data that are necessary.

$$t_{k+1}h = \min\left\{s_kh|\varepsilon^T(t)M\varepsilon(t) - \delta\bar{y}^T(t_kh)M\bar{y}(t_kh) > 0\right\}, \quad (4)$$

where $\varepsilon(t) = \bar{y}(s_kh) - \bar{y}(t_kh)$ with $s_kh = t_kh + \ell h$, and $\ell = 1, 2, \ldots, \bar{\ell}$.

Consider the following memory-based ETS filter used to estimate the measured output.

$$\begin{cases} \dot{x}_f(t) = \mathcal{A}_f x_f(t) + \mathcal{B}_f\bar{y}(t_kh) \\ z_f(t) = \mathcal{E}_f x_f(t). \end{cases} \quad (5)$$

Remark 2: In Fig. 3, the historical information over past period T is retained in AMO in this implementation, that is, $\bar{y}(t_kh)$ in the filter (5) includes the information over T, while the output information from $t_{(k-1)h}$ to t_kh is completely lost in the traditional sampling method.

Remark 3: The AMO in this brief is an average value over given past period T, while the historical information in [17], [18] is the average of m states at triggering instants. Therefore, more historical information is included in the AMO using our proposed scheme than in the traditional sampling method.

Remark 4: From (4), it can be seen that $\bar{y}(t_kh)$ is used as the input of the AMO-based ETS, while the conventional ETS uses the current sampling data $y(t_kh)$ as the ETS input. Accordingly, this method can weaken the sensitivity of the AMO-based ETS when the system is subjected to stochastic or abrupt disturbance, thus greatly reducing the number of unexpected triggering events.

Remark 5: From (3), it is apparent that, when $T \to 0$, the proposed AMO-based ETS reduces to a conventional ETS as in [19].

Define $\chi_k^\ell \triangleq [t_kh+(\ell-1)h+\tau_{\ell-1}, t_kh+\ell h+\tau_\ell)$ with $\tau_0 = \tau_{t_k}$ and $\tau_{\bar{\ell}} = \tau_{t_{k+1}}$, where τ_{t_k} is the network-induced delay with $0 \le \tau_{t_k} \le \bar{\tau}$. It is clear that $\cup_{\ell=1}^{\bar{\ell}}\chi_k^\ell = [t_k + \tau_{t_k}, t_{k+1} + \tau_{t_{k+1}})$.

Defining $\alpha_0(t) = t - s_kh$ for $t \in \chi_k^\ell$, it follows that

$$\begin{aligned} \bar{y}(t_kh) &= \bar{y}(t - \alpha_0(t)) - \varepsilon(t) \\ &\approx \frac{1}{6}\left[\sum_{i=0}^{2} y(t - \alpha_i(t)) + 3y(t - \alpha_1(t))\right] - \varepsilon(t), \end{aligned} \quad (6)$$

where $\alpha_1(t) = \alpha_0(t) + T/2, \alpha_2(t) = \alpha_0(t) + T$.

From the above discussion, it appears that $i \cdot T/2 \le \alpha_i(t) \le \bar{\alpha}_0 + i \cdot T/2 \triangleq \bar{\alpha}_i$ for $i = 0, 1, 2$ with $\bar{\alpha}_0 = h + \bar{\tau}$.

Combining (2), (5) and (6) yields the following filter error system:

$$\begin{cases} \dot{\varphi}(t) = \mathfrak{A}\varphi(t) + \mathfrak{D}x(t - \alpha_0(t)) + 4\mathfrak{D}x(t - \alpha_1(t)) \\ \qquad\quad +\mathfrak{D}x(t - \alpha_2(t)) + \mathfrak{B}_1\varepsilon(t) + \mathfrak{B}_2\omega(t) \\ e(t) = \mathfrak{E}\varphi(t), \end{cases} \quad (7)$$

for $t \in \chi_k^\ell$, where $\varphi(t) = [x^T(t) \quad x_f^T(t)]^T$, and

$$\mathfrak{A} = \begin{bmatrix} \mathcal{A} & 0 \\ 0 & \mathcal{A}_f \end{bmatrix}, \mathfrak{D} = \begin{bmatrix} 0 \\ \frac{1}{6}\mathcal{B}_f C \end{bmatrix}, \mathfrak{B}_1 = \begin{bmatrix} 0 \\ \mathcal{B}_f \end{bmatrix}, \mathfrak{B}_2 = \begin{bmatrix} \mathcal{B} \\ 0 \end{bmatrix},$$
$$\mathfrak{E} = \begin{bmatrix} \mathcal{E} & -\mathcal{E}_f \end{bmatrix}.$$

Before the filter design, recall Lemma 1, which is helpful in obtaining the filter parameters.

Lemma 1: For matrices $N \in \mathbb{R}^n$, $R \in \mathbb{R}^n$, $R > 0$ and $\begin{bmatrix} R & N^T \\ N & R \end{bmatrix} \ge 0$, and vector function $x : [\underline{\eta}, \overline{\eta}] \to \mathbb{R}^n$ such that the item $\int_{t-\overline{\eta}}^{t-\underline{\eta}} \dot{x}^T(s)R\dot{x}(s)ds$ in (8) is well defined, the following is obtained

$$-(\overline{\eta} - \underline{\eta})\int_{t-\overline{\eta}}^{t-\underline{\eta}} \dot{x}^T(s)R\dot{x}(s)ds \le -\begin{bmatrix} v_1 \\ v_2 \end{bmatrix}^T \begin{bmatrix} R & N^T \\ N & R \end{bmatrix}\begin{bmatrix} v_1 \\ v_2 \end{bmatrix},$$

where $v_1 = x(t - \underline{\eta}) - x(t - \eta(t))$, $v_2 = x(t - \eta(t)) - x(t - \overline{\eta})$.

III. Filtering of USVs Using the AMO-Based ETS

In this section, the AMO-based filter design for USVs is presented.

Theorem 1: For given scalars $T, \bar{\tau}, \beta$, and δ, the filtering error system in (7) is asymptotically stable with an H_∞ disturbance attenuation level γ, if there exist $P > 0$, $Q_i > 0$, $R_i > 0$ $M > 0$, and matrices T_i, S_{jk} $(i = 0, 1, 2;\ j, k = 1, 2)$ and S such that

$$\begin{bmatrix} \Omega_1 + \mathbf{He}\left\{\mathbb{H}_1^T\overline{\mathscr{A}}_1 + \beta\mathbb{H}_{12}^T\overline{\mathscr{A}}_2\right\} & \mathbb{H}_1^T\mathfrak{E}^T \\ \mathfrak{E}\mathbb{H}_1 & -I \end{bmatrix} \le 0, \quad (8)$$

$$\begin{bmatrix} R_i & T_i^T \\ T_i & R_i \end{bmatrix} > 0, \quad (9)$$

where

$$\begin{aligned} \Omega_1 &= \mathbf{He}\left\{\mathbb{H}_1^T P\mathbb{H}_{12}\right\} + \sum_{i=0}^{2}\mathbb{H}_1^T\mathbb{H}_0^T Q_i\mathbb{H}_0\mathbb{H}_1 \\ &\quad - \mathbb{H}_3^T Q_0\mathbb{H}_3 - \mathbb{H}_6^T Q_1\mathbb{H}_6 - \mathbb{H}_9^T Q_2\mathbb{H}_9 - \mathbb{H}_{10}^T M\mathbb{H}_{10} \\ &\quad + \sum_{i=0}^{2}\frac{T}{2}\mathbb{H}_{12}^T\mathbb{H}_0^T R_i\mathbb{H}_0\mathbb{H}_{12} - \frac{2}{T}\sum_{i=0}^{2}\mathcal{H}_i^T\mathcal{T}_i\mathcal{H}_i \\ &\quad + (\mathbb{H}_y - \mathbb{H}_{10})^T\delta M(\mathbb{H}_y - \mathbb{H}_{10}) \\ &\quad - \gamma^2\mathbb{H}_{11}^T\mathbb{H}_{11} - \mathbf{He}\left\{(\mathbb{H}_1^T S_1 + \beta\mathbb{H}_{12}^T S_2)\mathbb{H}_{12}\right\}, \\ \mathscr{A} &= [\mathfrak{A}\ \mathfrak{D}\ 0\ 0\ 4\mathfrak{D}\ 0\ 0\ \mathfrak{D}\ \mathfrak{B}_1\ \mathfrak{B}_2\ 0], \\ \overline{\mathscr{A}}_1 &= [\mathbb{A}_1\ \mathbb{D}\ 0\ 0\ 4\mathbb{D}\ 0\ 0\ \mathbb{D}\ \mathbb{B}_1\ \mathbb{B}_{21}\ 0], \\ \overline{\mathscr{A}}_2 &= [\mathbb{A}_2\ \mathbb{D}\ 0\ 0\ 4\mathbb{D}\ 0\ 0\ \mathbb{D}\ \mathbb{B}_1\ \mathbb{B}_{22}\ 0], \\ \mathbb{A}_1 &= \begin{bmatrix} S_{11}\mathcal{A} & \bar{A}_f \\ S_{12}\mathcal{A} & \bar{A}_f \end{bmatrix}, \mathbb{D} = \frac{1}{6}\begin{bmatrix} \overline{\mathcal{B}}_f C \\ \overline{\mathcal{B}}_f C \end{bmatrix}, \mathbb{B}_1 = \begin{bmatrix} \overline{\mathcal{B}}_f \\ \overline{\mathcal{B}}_f \end{bmatrix}, \\ \mathbb{A}_2 &= \begin{bmatrix} S_{21}\mathcal{A} & \bar{A}_f \\ S_{22}\mathcal{A} & \bar{A}_f \end{bmatrix}, \mathbb{B}_{21} = \begin{bmatrix} S_{11}\mathcal{B} \\ S_{12}\mathcal{B} \end{bmatrix}, \mathbb{B}_{22} = \begin{bmatrix} S_{21}\mathcal{B} \\ S_{22}\mathcal{B} \end{bmatrix}, \\ \mathbb{H}_0 &= [I_n\ 0_n], \mathbb{H}_y = \frac{1}{6}(\mathbb{H}_2 + 4\mathbb{H}_5 + \mathbb{H}_8), \\ \mathbb{H}_1 &= [I_{2n}\ 0_{2n\times(10n+m+n_\omega)}], \\ \mathbb{H}_j &= [0_{n\times jn}\ I_n\ 0_{n\times(11n-jn+m+n_\omega)}], \quad (j = 2, 3, \ldots, 9), \\ \mathbb{H}_{10} &= [0_{m\times 10n}\ I_m\ 0_{m\times n_\omega}\ 0_{m\times 2n}], \\ \mathbb{H}_{11} &= [0_{n_\omega\times 10n}\ 0_{n_\omega\times m}\ I_{n_\omega}\ 0_{n_\omega\times 2n}], \\ \mathbb{H}_{12} &= [0_{2n\times 10n}\ 0_{2n\times(m+n_\omega)}\ I_{2n}], \\ \mathcal{H}_0 &= \begin{bmatrix} \mathbb{H}_0\mathbb{H}_1 - \mathbb{H}_2 \\ \mathbb{H}_2 - \mathbb{H}_3 \end{bmatrix}, \mathcal{H}_1 = \begin{bmatrix} \mathbb{H}_4 - \mathbb{H}_5 \\ \mathbb{H}_5 - \mathbb{H}_6 \end{bmatrix}, \\ \mathcal{H}_2 &= \begin{bmatrix} \mathbb{H}_7 - \mathbb{H}_8 \\ \mathbb{H}_8 - \mathbb{H}_9 \end{bmatrix}, \ \mathcal{T}_i = \begin{bmatrix} R_i & T_i^T \\ T_i & R_i \end{bmatrix}, (i = 0, 1, 2). \end{aligned}$$

Moreover, the filter parameters in (7) are given as $\mathcal{A}_f = S^{-1}\bar{A}_f$, $\mathcal{B}_f = S^{-1}\bar{\mathcal{B}}_f$, $\mathcal{E}_f = \mathcal{E}_f$.

Proof: For convenience of prescription, we define $\phi_i^T(t) = [x^T(t - i \cdot T/2) \;\; x^T(t - \alpha_i(t)) \;\; x^T(t - \bar{\alpha}_i)]$ with $i = 0, 1, 2$ and $\phi^T(t) = [\varphi^T(t) \;\; x^T(t - \alpha_0(t)) \;\; x^T(t - \bar{\alpha}_0) \;\; \phi_1^T(t) \;\; \phi_2^T(t) \;\; \varepsilon^T(t) \;\; \omega^T(t) \;\; \dot{\varphi}^T(t)]$.

System (7) can then be rewritten as

$$\dot{\varphi}(t) = \mathscr{A}\phi(t) \tag{10}$$

For the Lyapunov functional

$$V(t) = V_1(t) + V_2(t) + V_3(t), \tag{11}$$

where

$$\begin{aligned} V_1(t) &= \varphi^T(t)P\varphi(t), \\ V_2(t) &= \sum_{i=0}^{2}\int_{t-\bar{\alpha}_i}^{t} x^T(t)Q_i x(t), \\ V_3(t) &= \sum_{i=0}^{2}\int_{t-\bar{\alpha}_i}^{t-i\cdot T/2}\int_{s}^{t} x^T(v)R_i x(v)dvds, \end{aligned}$$

we find that

$$\begin{aligned} \dot{V}_1(t) &= 2\varphi^T(t)P\mathbb{H}_{12}\phi(t), \\ \dot{V}_2(t) &= \sum_{i=0}^{2} x^T(t)Q_i x(t) - \sum_{i=0}^{2} x^T(t-\bar{\alpha}_i)Q_i x(t-\bar{\alpha}_i), \\ \dot{V}_3(t) &= \sum_{i=0}^{2}\frac{T}{2}\dot{x}^T(t)R_i\dot{x}(t) - \sum_{i=0}^{2}\int_{t-\bar{\alpha}_i}^{t-i\cdot T/2}\dot{x}^T(v)R_i\dot{x}(v)dv \end{aligned}$$

From Lemma 1 and (7), the following can be obtained:

$$\begin{aligned} \dot{V}(t) \le\; & 2\phi^T(t)\mathbb{H}_1^T P\mathbb{H}_{12}\phi(t) + \sum_{i=0}^{2}\phi^T(t)\mathbb{H}_1^T\mathbb{H}_0^T Q_i\mathbb{H}_0\mathbb{H}_1\phi(t) \\ & - \phi^T(t)(\mathbb{H}_3^T Q_0\mathbb{H}_3 + \mathbb{H}_6^T Q_1\mathbb{H}_6 + \mathbb{H}_9^T Q_2\mathbb{H}_9)\phi(t) \\ & + \sum_{i=0}^{2}\phi^T(t)\frac{T}{2}\mathbb{H}_{12}^T\mathbb{H}_0^T R_i\mathbb{H}_0\mathbb{H}_{12}\phi(t) \\ & - \frac{2}{T}\sum_{i=0}^{2}\begin{bmatrix} v_{1i} \\ v_{2i}\end{bmatrix}^T\begin{bmatrix} R_i & * \\ T_i & R_i\end{bmatrix}\begin{bmatrix} v_{1i} \\ v_{2i}\end{bmatrix} - \phi^T(t)\mathbb{H}_{10}^T M\mathbb{H}_{10}\phi(t) \\ & + \phi^T(t)(\mathbb{H}_y - \mathbb{H}_{10})^T\delta M(\mathbb{H}_y - \mathbb{H}_{10})\phi(t) \\ & + 2\phi^T(t)(\mathbb{H}_1^T S_1 + \beta\mathbb{H}_{12}^T S_2)(\mathscr{A} - \mathbb{H}_{12})\phi(t) \\ & + \phi^T(t)[\mathbb{H}_1^T\mathfrak{E}^T\mathfrak{E}\mathbb{H}_1 - \gamma^2\mathbb{H}_{11}^T\mathbb{H}_{11}]\phi(t) \\ & - e^T(t)e(t) + \gamma^2\omega^T(t)\omega(t), \end{aligned}$$

where $v_{1i} = x(t - i \cdot T/2) - x(t - \alpha_i(t))$, $v_{2i} = x(t - \alpha_i(t)) - x(t - \bar{\alpha}_i)$.

We then have

$$\begin{aligned} \dot{V}(t) + \mathcal{J}(t) \le\; & \phi^T(t)\big\{\Omega_1 + \mathbb{H}_1^T\mathfrak{E}^T\mathfrak{E}\mathbb{H}_1 \\ & + \mathbf{He}\big\{(\mathbb{H}_1^T S_1 + \beta\mathbb{H}_{12}^T S_2)\mathscr{A}\big\}\big\}\phi(t) \end{aligned} \tag{12}$$

with $\mathcal{J}(t) = e^T(t)e(t) - \gamma^2\omega^T(t)\omega(t)$.

Defining $S_1 = \begin{bmatrix} S_{11} & S \\ S_{12} & S\end{bmatrix}$, $S_2 = \begin{bmatrix} S_{21} & S \\ S_{22} & S\end{bmatrix}$, $\bar{\mathcal{A}}_f = S\mathcal{A}_f$, and $\bar{\mathcal{B}}_f = S\mathcal{B}_f$ and using the Schur complement for (8) yield that

$$\dot{V}(t) + \mathcal{J}(t) \le 0. \tag{13}$$

TABLE I
DATA RELEASING RATE UNDER THE PROPOSED AMO-BASED ETS

Window scale	T=0.03	T=0.06	T=0.10
Data releasing rate	11.6%	11.3%	10.9%

Therefore, for $\omega(t) = 0$, one can know that the system (7) is asymptotically stable due to $\dot{V}(t) \le 0$ and, under zero initial condition, it satisfies $\int_{t_0}^{\infty} e^T(s)e(s)ds \le \int_{t_0}^{\infty}\gamma^2\omega^T(s)\omega(s)ds$ with $\omega(t) \ne 0$. This completes the proof. ■

IV. EXAMPLE

To illustrate the benefits of the proposed approach, we consider a USV with the same parameters as in [20]. The matrices in (1) are given as

$$A = \begin{bmatrix} 0 & 0 & 1 & 0 & 0 \\ 0 & 0 & 0 & 1 & 0 \\ -2.6569 & 0 & -6.7938 & 0 & 2.1202 \\ 0 & 0 & 0 & -2.3747 & -1.0924 \\ 0 & 0 & 0 & 0 & -1.9001 \end{bmatrix},$$

$$B = \begin{bmatrix} 0 \\ 0 \\ -0.0537 \\ -0.0245 \\ 0.0722 \end{bmatrix}, \quad \mathcal{B} = \begin{bmatrix} 0 & 0 \\ 0 & 0 \\ 2.6569 & 0 \\ 0 & 0 \\ 0 & 2.3747 \end{bmatrix}.$$

The controller $K = [1.1118, 3.465, 6.6327, -1.5691, 3.1662]$ is employed to stabilize the system, while the other matrices are given as

$$\begin{aligned} \mathcal{C} &= \begin{bmatrix} 0 & 10 & 0 & 10 & 10 \end{bmatrix}, \\ \mathcal{E} &= \begin{bmatrix} 0 & 0 & 1 & 1 & 1 \end{bmatrix}. \end{aligned}$$

The upper bounds for the communication delay and the sampling time are $\bar{\tau} = 0.1s$ and $h = 0.025s$, respectively. For $\delta = 0.01$, $\beta = 0.01$, $T = 0.1s$, and $\gamma = 20$, the filter gains and the triggering parameter can be derived from Theorem 1 as

$$\mathcal{A}_f = \begin{bmatrix} -0.4240 & -0.0448 & 0.1855 & -0.2855 & -0.1719 \\ -0.2010 & -0.1063 & -0.1418 & 0.4510 & -0.1629 \\ -3.3132 & -0.1299 & -9.0414 & 0.3691 & 1.3221 \\ 0.2707 & -0.2268 & 0.9869 & -2.2573 & -0.2808 \\ -0.8724 & 0.6712 & -4.6943 & 3.1253 & -2.1854 \end{bmatrix},$$

$$\mathcal{B}_f = \begin{bmatrix} -0.0045 \\ -0.0090 \\ -0.0378 \\ 0.0040 \\ -0.0620 \end{bmatrix}, \quad \mathcal{E}_f = \begin{bmatrix} -6.4165 \\ 0.5078 \\ -16.8881 \\ 0.5740 \\ -5.3277 \end{bmatrix}^T, \quad M = 476.4499.$$

The wave-induced disturbance for heading and rudder anger is assumed as $\omega(t) = e^{-0.25t}[sin(0.5\pi t) + v_1(t), \;\; sin(0.5\pi t) + v_2(t)]^T$ for $t \in [0, \; 10s]$, and $\omega(t) = [0, \;\; 0]^T$ for the remaining time, where $v_i(t)$ is a stochastic variable subject to $|v_i(t)| \le 2$ for $i = 1, 2$.

The responses of the measured output $z(t)$ and filter output $z_f(t)$ and the corresponding triggering sequence are shown in Fig. 4 and Fig. 5, respectively. The case in Fig. 4 is a

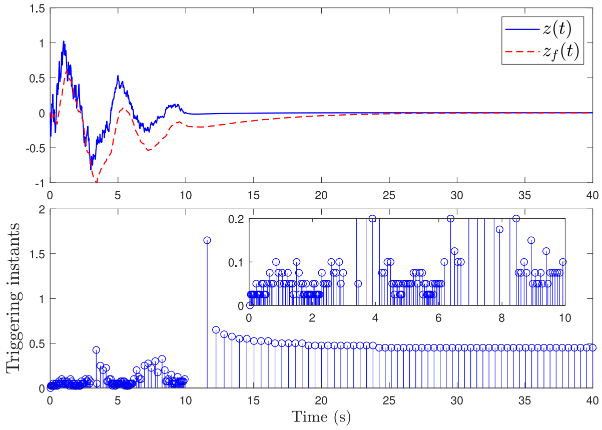

Fig. 4. Responses of the measured output $z(t)$ and filtering output $z_f(t)$ and the triggering sequence under a conventional ETS.

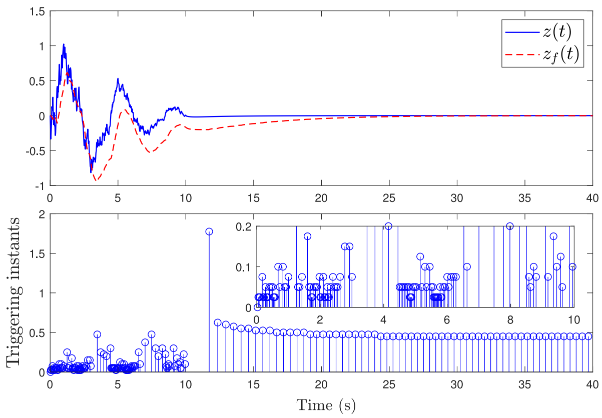

Fig. 5. Responses of the measured output $z(t)$ and filtering output $z_f(t)$ and the triggering sequence under the proposed AMO-based ETS.

USV system with a conventional ETS, while Fig. 5 presents a system using the proposed AMO-based ETS with T = 0.10. It can be clearly observed that the volume of signal transmissions for the proposed AMO-based ETS is lower than that for the conventional ETS. Table I presents the releasing rate under the proposed AMO-based ETS with different window scales, showing that some unexpected sampling data is prevented from being transmitted over the network. Moreover, a larger T has the potential to generate a lower releasing rate.

V. Conclusion

In this brief, an AMO-based ETS is established for the filtering of networked USVs. Under the proposed AMO-based ETS, the transmitted sampling data includes historical information, while the output information of the plant between adjacent sampling instants is lost. Therefore, the filtering performance of USVs is improved. Furthermore, a lower the data releasing rate is achieved by using the proposed AMO-based ETS, especially for systems subject to stochastic noise and disturbance. The presented simulation results illustrate the advantages of the proposed method. In the future research, we will extend our method to the filtering design of networked systems subject to cyber-attacks.

References

[1] Z. Zuo, C. Liu, Q.-L. Han, and J. Song, "Unmanned aerial vehicles: Control methods and future challenges," *IEEE/CAA J. Automatica Sinica*, vol. 9, no. 4, pp. 601–614, Apr. 2022, doi: 10.1109/JAS.2022.105410.

[2] W. Zhou, Y. Wang, C. K. Ahn, J. Cheng, and C. Chen, "Adaptive fuzzy backstepping-based formation control of unmanned surface vehicles with unknown model nonlinearity and actuator saturation," *IEEE Trans. Veh. Technol.*, vol. 69, no. 12, pp. 14749–14764, Dec. 2020.

[3] N. Wang, Y. Gao, H. Zhao, and C. K. Ahn, "Reinforcement learning-based optimal tracking control of an unknown unmanned surface vehicle," *IEEE Trans. Neural Netw. Learn. Syst.*, vol. 32, no. 7, pp. 3034–3045, Jul. 2021.

[4] Z. Liu, Y. Zhang, C. Yuan, and J. Luo, "Adaptive path following control of unmanned surface vehicles considering environmental disturbances and system constraints," *IEEE Trans. Syst., Man, Cybern., Syst.*, vol. 51, no. 1, pp. 339–353, Jan. 2021.

[5] Z. Peng, Y. Jiang, and J. Wang, "Event-triggered dynamic surface control of an underactuated autonomous surface vehicle for target enclosing," *IEEE Trans. Ind. Electron.*, vol. 68, no. 4, pp. 3402–3412, Apr. 2021.

[6] R. Cui, L. Chen, C. Yang, and M. Chen, "Extended state observer-based integral sliding mode control for an underwater robot with unknown disturbances and uncertain nonlinearities," *IEEE Trans. Ind. Electron.*, vol. 64, no. 8, pp. 6785–6795, Aug. 2017.

[7] S. Wang, M. Fu, and Y. Wang, "Robust adaptive steering control for unmanned surface vehicle with unknown control direction and input saturation," *Int. J. Adapt. Control Signal Process.*, vol. 33, no. 7, pp. 1212–1224, 2019.

[8] B. Zhang, H. Du, J. Lam, N. Zhang, and W. Li, "A novel observer design for simultaneous estimation of vehicle steering angle and sideslip angle," *IEEE Trans. Ind. Electron.*, vol. 63, no. 7, pp. 4357–4366, Jul. 2016.

[9] X. Ge, Q.-L. Han, L. Ding, Y.-L. Wang, and X.-M. Zhang, "Dynamic event-triggered distributed coordination control and its applications: A survey of trends and techniques," *IEEE Trans. Syst., Man, Cybern., Syst.*, vol. 50, no. 9, pp. 3112–3125, Sep. 2020.

[10] G. Zong, H. Ren, and H. R. Karimi, "Event-triggered communication and annular finite-time H_∞ filtering for networked switched systems," *IEEE Trans. Cybern.*, vol. 51, no. 1, pp. 309–317, Jan. 2021.

[11] Z. Gu, D. Yue, J. H. Park, and X. Xie, "Memory-event-triggered fault detection of networked IT2 T–S fuzzy systems," *IEEE Trans. Cybern.*, early access, Mar. 14, 2022, doi: 10.1109/TCYB.2022.3155755.

[12] X. Ge, S. Xiao, Q.-L. Han, X.-M. Zhang, and D. Ding, "Dynamic event-triggered scheduling and platooning control co-design for automated vehicles over vehicular ad-hoc networks," *IEEE/CAA J. Automatica Sinica*, vol. 9, no. 1, pp. 31–46, Jan. 2022.

[13] X. Wang and M. D. Lemmon, "Event-triggering in distributed networked control systems," *IEEE Trans. Autom. Control*, vol. 56, no. 3, pp. 586–601, Mar. 2011.

[14] H. Yu and F. Hao, "Input-to-state stability of integral-based event-triggered control for linear plants," *Automatica*, vol. 85, pp. 248–255, Nov. 2017.

[15] S. Yan, Z. Gu, and C. K. Ahn, "Memory-event-triggered H_∞ filtering of unmanned surface vehicles with communication delays," *IEEE Trans. Circuits Syst. II, Exp. Briefs*, vol. 68, no. 7, pp. 2463–2467, Apr.–Jun. 2021.

[16] K. E. Atkinson, *An Introduction to Numerical Analysis*, 2nd ed. New York, NY, USA. Wiley, 2008.

[17] E. Tian and C. Peng, "AMO-based event-triggering H_∞ load frequency control for power systems under deception attacks," *IEEE Trans. Cybern.*, vol. 50, no. 11, pp. 4610–4618, Nov. 2020.

[18] X. Guo, D. Zhang, J. Wang, and C. K. Ahn, "Adaptive memory event-triggered observer-based control for nonlinear multi-agent systems under DoS attacks," *IEEE/CAA J. Automatica Sinica*, vol. 8, no. 10, pp. 1644–1656, Oct. 2021.

[19] D. Yue, E. Tian, and Q.-L. Han, "A delay system method for designing event-triggered controllers of networked control systems," *IEEE Trans. Autom. Control*, vol. 58, no. 2, pp. 475–481, Feb. 2013.

[20] X. Wang, Z. Fei, H. Gao, and J. Yu, "Integral-based event-triggered fault detection filter design for unmanned surface vehicles," *IEEE Trans. Ind. Informat.*, vol. 15, no. 10, pp. 5626–5636, Oct. 2019.